Journal of Laser Applications

Novel laser-based metasurface fabrication process for transparent conducting surfaces

Cite as: J. Laser Appl. **31**, 022505 (2019); https://doi.org/10.2351/1.5096085
Submitted: 14 March 2019 . Accepted: 14 March 2019 . Published Online: 05 April 2019

Qinghua Wang, Bao-jia Li, Fatima Toor, and Hongtao Ding

Journal of Laser Applications ARTICLE scitation.org/journal/jla

Novel laser-based metasurface fabrication process for transparent conducting surfaces

Cite as: J. Laser Appl. 31, 022505 (2019); doi: 10.2351/1.5096085
Submitted: 14 March 2019 · Accepted: 14 March 2019 ·
Published Online: 5 April 2019

Qinghua Wang,[1] Bao-jia Li,[1,2,3] Fatima Toor,[4] and Hongtao Ding[1]

AFFILIATIONS

[1]Department of Mechanical Engineering, University of Iowa, Iowa City, Iowa 52242
[2]School of Materials Science and Engineering, Jiangsu University, Zhenjiang 212013, People's Republic of China
[3]Jiangsu Provincial Key Laboratory of Center for Photon Manufacturing Science and Technology, Jiangsu University, Zhenjiang 212013, People's Republic of China
[4]Department of Electrical and Computer Engineering, University of Iowa, Iowa City, Iowa 52242

ABSTRACT

Transparent conducting film provides key functions for various optoelectronic devices. Existing manufacturing processes of a transparent conducting film are usually very costly in terms of materials or processing time. The goal of this research is to develop a new surface engineering method for low-cost and high-throughput fabrication of large-size, transparent conducting glass windows. A novel laser-based metasurface fabrication process is presented in this work, which comprises two steps: (1) evaporating the glass substrate by an ultrathin metal film with a thickness on the order of 10 nm and (2) laser patterning the coated surface using a nanosecond pulsed laser (1064 nm wavelength) with a typical feature size of hundreds of micrometers. During the second step of the laser scanning process using an appropriate pulse energy density, the metal film absorbs most of the laser pulse energy and is patterned through laser material ablation, while little damage will be induced on the substrate since its absorptivity at the laser wavelength is low. Experimental results have shown that a transparent conducting film with an average visible transmittance of ~67% and a sheet resistance of ~20 Ω/sq can be successfully fabricated. Compared with the other existing methods, this novel laser surface patterning process significantly improves the processing efficiency and reduces the production cost that renders practical treatment of glass materials or transparent ceramics to produce transparent conducting surfaces.

Key words: laser-based metasurface fabrication, ultrathin film, microhole array, visible transmittance, electrical conductivity

 https://doi.org/10.2351/1.5096085

I. INTRODUCTION

A transparent conducting film plays a key role in many optoelectronic devices such as liquid-crystal displays, organic light-emitting diodes (OLEDs), photocells, and touch-screen panels. The need for large-area flexible devices has been continuously growing. Conventionally, indium tin oxide (ITO), which is a type of wide bandgap transparent conductive oxides (TCOs), has been the most extensively used material for transparent conducting films due to its excellent optical transparency in visible spectra and high electrical conductivity. However, ITO has several key drawbacks, including high scarcity, large amount of waste of target material, and the nature of fragility,[1] which are adverse for treating large-size glass panels. In view of the above-mentioned limitations of ITO, many alternative materials such as carbon nanotubes (CNTs),[2,3] graphene,[4,5] doped zinc oxide (ZnO) based TCOs,[6,7] metal [silver (Ag), copper (Cu)] nanowires (NWs),[8,9] metal microgrids,[10,11] and graphene–Ag NW hybrid materials[12] have been investigated. However, these materials all have their own drawbacks. For example, carbon-based nanomaterials, such as CNTs or graphene, exhibit relatively poor photoelectric properties compared with ITO.[13]

Various fabrication methods have also been attempted by researchers, including laser sintering, electrospinning, inkjet printing, photolithography, and nanoimprinting. Hong *et al.*[14] introduced a novel approach to fabricate a metallic grid based transparent conductor by direct selective laser sintering of Ag nanoparticle (NP) ink, which had low sheet resistance and high transmittance on a large scale. Consistent Ag conductor microlines were fabricated over a wafer-scale large area by using a focused laser as a localized heat source. Wu *et al.*[15] presented a facile fabrication process for a new kind of transparent conducting electrode that exhibited superior optoelectronic performances and remarkable mechanical flexibility under both stretching and bending stresses. The electrode was

composed of a free-standing metallic nanotrough network and was produced with a process combining electrospinning and metal deposition. Jeong *et al.*[16] reported the characteristics of Ag grid/ITO hybrid transparent electrodes fabricated by an inkjet printing method. By inserting an inkjet-printed Ag grid between inkjet-printed ITO electrodes, the high sheet resistance limitation of inkjet-printed ITO electrodes was overcome. In addition, it was found that control of the Ag grid separation distance is a key parameter in determining the figure of merit value of the hybrid transparent electrodes, which was consistent with the calculated values. Photolithography has also been used by several researchers to create the patterns of metal grids.[17,18] The fabricated nanopattern-based transparent conducting film exhibited high visible transmittance and low sheet resistance. Kang and Guo[19] utilized nanoimprint lithography to fabricate a semitransparent metal electrode in the form of a nanometer-scale periodically perforated metal film that showed high optical transmittance in the visible spectrum as well as excellent electrical conductivity. However, all of these above-mentioned fabrication methods are either too time-consuming or too costly. There is a strong need for a new technology applicable for time-efficient and cost-effective fabrication methods of large-area transparent conducting films.

Direct fabrication of transparent conducting films using laser has been a newly emerging method that can be both time-efficient and cost-effective. Li *et al.*[20–31] have conducted an extensive research work on improving the photoelectric properties of single-layer films and bilayer or trilayer composite films using laser annealing and laser texturing methods. By irradiation using a nanosecond pulsed laser with a wavelength of 532 nm, they have enhanced the photoelectric properties of fluorine doped tin oxide (FTO) single-layer films,[20] aluminum (Al) doped zinc oxide (AZO)/FTO,[21] textured metal (Al, Ag, Cu)/FTO,[22] Ag/FTO,[23] textured platinum (Pt)/FTO,[24] and titanium dioxide (TiO_2)/FTO (Ref. 25) bilayer composite films, AZO/Ag/FTO (Ref. 26) and AZO/Pt/FTO (Ref. 27) trilayer composite films. They also improved the laser annealing process by adding an external magnetic field,[28–30] which can greatly promote grain growth and increase grain size in films, thereby effectively enhance transmittance and reduce sheet resistance. They also sputtered AZO layers on polyethylene terephthalate (PET) flexible substrates and annealed the AZO/PET flexible films using a 532 nm nanosecond pulsed laser. This method shows effectiveness in enhancing grain crystallinity, increasing crystallite size, and avoiding damage to the PET flexible substrates, thus can effectively enhance visible transmittance and electrical conductivity of the films.[31] However, either FTO or AZO layer was used for film preparation in these studies, which will increase the production cost of the transparent conducting films. Paeng *et al.*[32] produced Cu flexible transparent conducting electrodes (FTCEs) by nanosecond (ns) laser ablation exhibiting a sheet resistance of 17.48 Ω/sq and an optical transmittance at a wavelength of 550 nm of 83%, which shows a significantly better performance than commercial ITO films. The nanosecond laser ablation of ultrathin Cu films facilitated material removal without introducing thermal damage on the polymer substrates. As a result, metallic hole array structures were directly produced on different heat-sensitive flexible substrates. The Cu FTCEs showed a good mechanical durability in bending, squeezing, and twisting tests. A touch-screen panel was demonstrated using the fabricated transparent conducting electrodes. However, the processing efficiency of the laser ablation method in their work is extremely low since a very small laser beam diameter on the level of several micrometers (<10 μm) was utilized. It will take more than 4 h to process a 36×36 mm^2 area using their experimental method. This will make it impossible to scale up the process.

In this work, a novel laser-based metasurface fabrication (LMF) process is developed as a new surface engineering method for low-cost and high-throughput fabrication of large-scale transparent conducting films with glass as the substrate material. The laser-patterned transparent conducting film exhibits combined properties of high visible transmittance and low sheet resistance. This novel laser surface patterning process significantly improves the processing efficiency and reduces production cost that provides a new avenue for production of transparent conducting films.

II. EXPERIMENT

A. LMF process development

As shown in Fig. 1, the LMF process comprises two steps: (1) coating the glass substrate by an ultrathin metal film with a thickness on the order of 10 nm; (2) fabricating a microhole array on the metal film by laser patterning using a nanosecond pulsed laser (1064 nm wavelength) with a typical laser beam diameter on the order of ~150 μm.

Pure Cu was used as the target material in the first step. For coating the glass substrate with Cu films, the Cu target was evaporated and deposited using the E-beam evaporation technique. The deposition facility used was an Angstrom Engineering 6-pocket E-Beam Evaporator system. During the E-beam evaporation process, the thickness of the deposited metal was monitored *in situ* by a thickness monitor.

LMF employed a Q-Switched Nd:YAG nanosecond laser (1064 nm wavelength, Quanta-Ray Lab-150-10, Spectra-Physics) with a pulse duration of 120 ns, a pulse energy on the order of hundreds of milliJoules, and a repetition rate of 10 Hz. A 3-axis galvanometer laser scanner (SCANLAB intelliSCAN® 20 and varioSCANde 40i), configured with an f-theta objective, served to direct a laser beam onto the sample. The nanosecond laser patterning of thin metal films directly produced hole arrays without inducing thermal damage on the underlying glass substrate. The scanning speed and line spacing were controlled using the SCANLAB control software. The current process used a line spacing of ~150 μm and a scanning speed of ~1.5 mm/s. By varying these two parameters, the areal density, defined as the ratio of residual area after the LMF process over the total area, could be adjusted. Figure 2 shows a 36×36 mm^2 laser-patterned area on a Cu film obtained using the LMF process. The laser-patterned area shows higher optical transmittance than the pure metal film and demonstrates good electrical conductivity as well. It should be noted that this work used just a 10 Hz nanosecond laser which affected the processing efficiency. The scanning speed can be substantially increased by adopting higher pulse repetition lasers. This 36×36 mm^2 laser-patterned area could be obtained within 6 s using a laser at 10 kHz pulse. This will enable large-area processing for industrial applications.

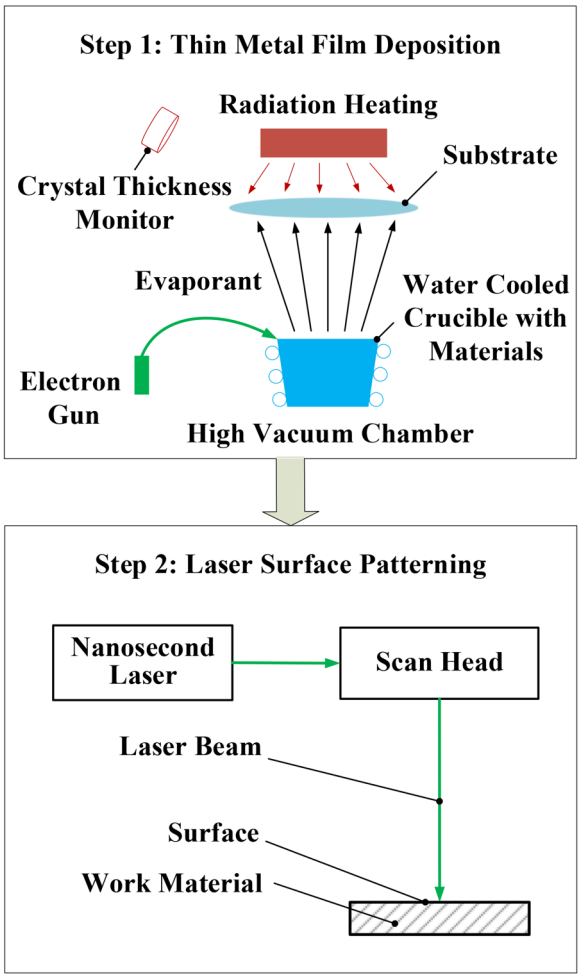

FIG. 1. Schematic of the LMF process.

B. Sheet resistance measurement

Sheet resistance is a measure of the electrical conductivity of thin films that are nominally uniform in thickness and is applicable to two-dimensional systems in which thin films are considered as two-dimensional entities. The lower the sheet resistance, the better the electrical conductivity thin films will possess. In a regular three-dimensional conductor, the sheet resistance can be defined using the following equation:

$$R = \rho \frac{L}{A} = \rho \frac{L}{Wt}, \tag{1}$$

where ρ is the resistivity, A is the cross-sectional area, and L is the length. The cross-sectional area can be calculated by the width W and the sheet thickness t.

The sheet resistance of the laser-patterned hole array was tested with a digital four point probe sheet resistivity measurement system (Signatone Pro4 series), which is connected to a sourcemeter

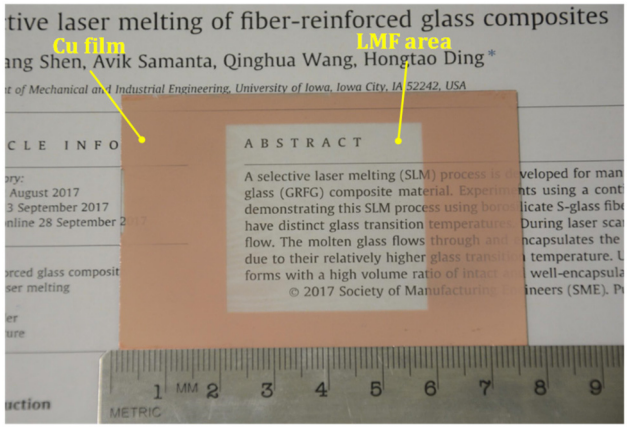

FIG. 2. A large transparent conducting film produced by the LMF process is placed on the text of a research paper illustrating its high visible transmittance. The size of the LMF area is 36 × 36 mm^2.

(Keithley 2400 series) for sheet resistance value reading. The schematic for sheet resistance measurement is shown in Fig. 3. Four metallic lined up probe pins were applied to the surface of a specimen, and current was made to flow through the two outermost probe pins. The difference in potential between the two intermediate probe pins was measured. The actual sheet resistance can be calculated using the following equation:

$$\rho s = \frac{V}{I}\frac{\pi}{\ln 2} = 4.5325\frac{V}{I}, \tag{2}$$

where ρs is the sheet resistance with the unit of Ω/sq, V is the voltage between the inner probes, and I is the current through the outer probes. S shown in Fig. 3 is the needle spacing.

Each specimen surface was measured for multiple (typically three) times at various locations, and the averaged value of these sheet resistance measurements was reported.

C. Optical transmittance measurement

Optical transmittance of a material refers its effectiveness in transmitting radiant energy. It is defined as the fraction of incident

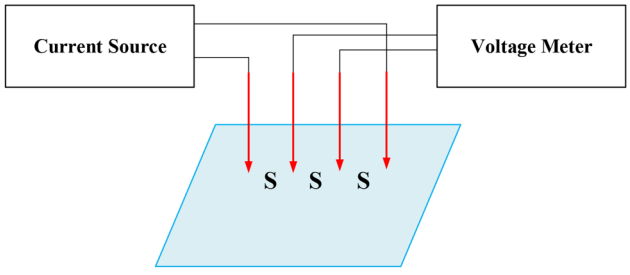

FIG. 3. Schematic for sheet resistance measurement.

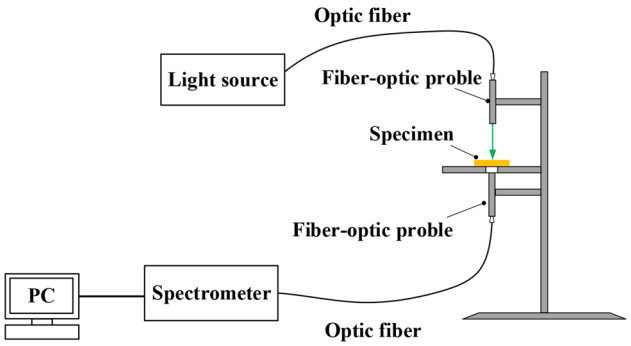

FIG. 4. Experimental setup for optical transmittance measurement.

electromagnetic power that is transmitted through a material surface. Hemispherical transmittance of a surface, denoted as T, is defined in the following equation:

$$T = \frac{\Phi_e^t}{\Phi_e^i}, \tag{3}$$

where Φ_e^t is the radiant flux transmitted by that surface and Φ_e^i is the radiant flux received by that surface.

The optical transmittance of the laser-patterned microhole array was measured using a UV-Vis spectrometer (USB4000, Ocean Optics Co.) with normal incidence. The UV-Vis spectrometer measures the transmittance of the specimen surface in the wavelength range of 400–1000 nm. Before transmittance measurement, calibration of the transmittance scale was performed by measuring the transmittance through air. Then, the specimen was placed on the optical path of normal incidence for the actual transmittance measurement. During the transmittance measurement, light from a visible and near-infrared light source (LH-2000, Ocean Optics Co.) was fed through the illuminating fiber-optic probe, directed through the specimen placed on top of the pinhole, and into the quartz fiber-optic probe coupled to a USB4000 spectrometer. OCEANVIEW® software was utilized to process and visualize the transmittance measurement results. Each specimen surface was measured for multiple (typically three) times at various locations, and the averaged spectral transmittance was obtained. The schematic for optical transmittance measurement is shown in Fig. 4.

III. RESULTS AND DISCUSSION

A. Electrical conductivity

The sheet resistance for as-prepared Cu films with different Cu layer thicknesses and 8-nm-thick laser-patterned Cu thin films with different areal densities is shown in Fig. 5. For the as-prepared Cu film, as the film thickness increased from 6.5 to 15 nm, the sheet resistance gradually decreased from 11.0 to 2.4 Ω/sq, as shown in Fig. 5(a). After the LMF process, the sheet resistance of the 8-nm-thick laser-patterned Cu thin film varied with areal density. As the areal density increased from 32% to 56%, the sheet resistance decreased from 21.7 to 10.9 Ω/sq, as shown in Fig. 5(b).

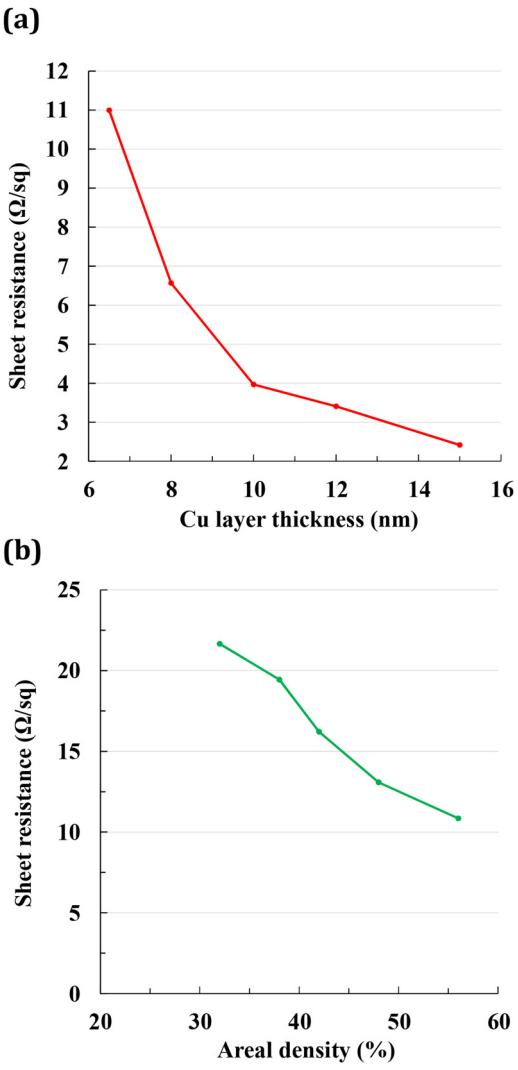

FIG. 5. Sheet resistance of (a) the as-prepared Cu film (without laser patterning) as a function of Cu layer thickness and (b) the 8-nm-thick laser-patterned Cu thin film as a function of areal density.

Compared with the as-prepared Cu film, the sheet resistance of the 8-nm-thick laser-patterned Cu film increased as a considerable amount of metal was removed during laser patterning. However, the increase is not significant but rather still within a reasonable range. The ultrathin metal film with a sheet resistance on the order of ~20 Ω/sq can still be used for various applications, such as OLED circuits and touch-screen panels.

B. Visible transmittance

The as-prepared ultrathin metal film should be semitransparent in order to achieve high visible transmittance after laser patterning. Cu films with thicknesses of 15, 12, 10, 8, and 6.5 nm were deposited

on the glass substrates. The as-prepared Cu film with a thickness of 15 nm only has an average visible transmittance (in the visible wavelength range of 450–800 nm for this work) of 23.8%. When the thickness of Cu film was reduced to 10 and 8 nm, the average visible transmittance increased to 37.7% and 50.1%, respectively. With the thickness of Cu film further reduced to 6.5 nm, the average visible transmittance increased further to 55.7%, as shown in Fig. 6(a). According to literature data,[33] it is believed that the Cu film thickness can be further reduced to ensure that the as-prepared Cu film has an average visible transmittance of ~60% in the visible wavelength range of 450–800 nm with satisfying sheet resistance. However, the sheet resistance of the as-prepared Cu film with very low film thickness will be extraordinarily high, which will affect the electrical conductivity of laser-patterned films. Thus, in order to maintain balance between the sheet resistance and visible transmittance on the as-deposited film, the film thickness should not be too low.

The average visible transmittance increases as areal density decreases, as shown in Fig. 6(b). Using a laser spot size of 140 μm, a scanning speed of 1.5 mm/s, a pitch of 150 μm, and an areal density of 32%, an average visible transmittance of 67.2% and a sheet resistance of 21.7 Ω/sq can be achieved on the 8-nm-thick Cu thin film. The average visible transmittance of the as-prepared Cu thin film is 50.1%. The LMF process increases the average visible transmittance by 17.1%. An optical image of the laser-patterned microhole array pattern is shown in Fig. 7(a). From the optical image of the patterned hole array, it can be found that there are burrs generated around the hole circumference after the LMF process. These burrs should be attributed to the high laser fluence used in the experiments that generated distinct heat-affected zones. More details of the burrs can be found in the 3D surface profile of

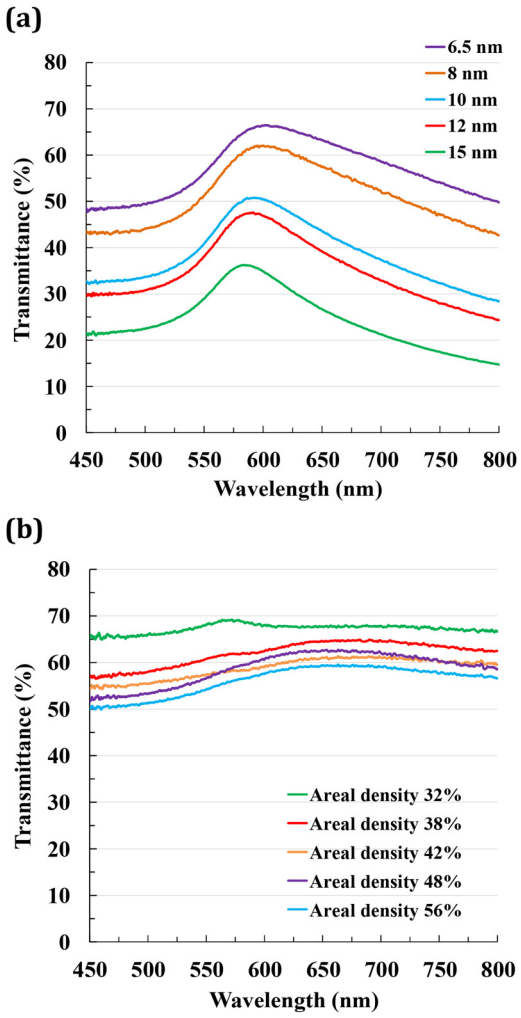

FIG. 6. Visible transmittance of (a) the as-prepared Cu film (without laser patterning) as a function of Cu layer thickness and (b) the 8-nm-thick laser-patterned Cu thin film as a function of areal density.

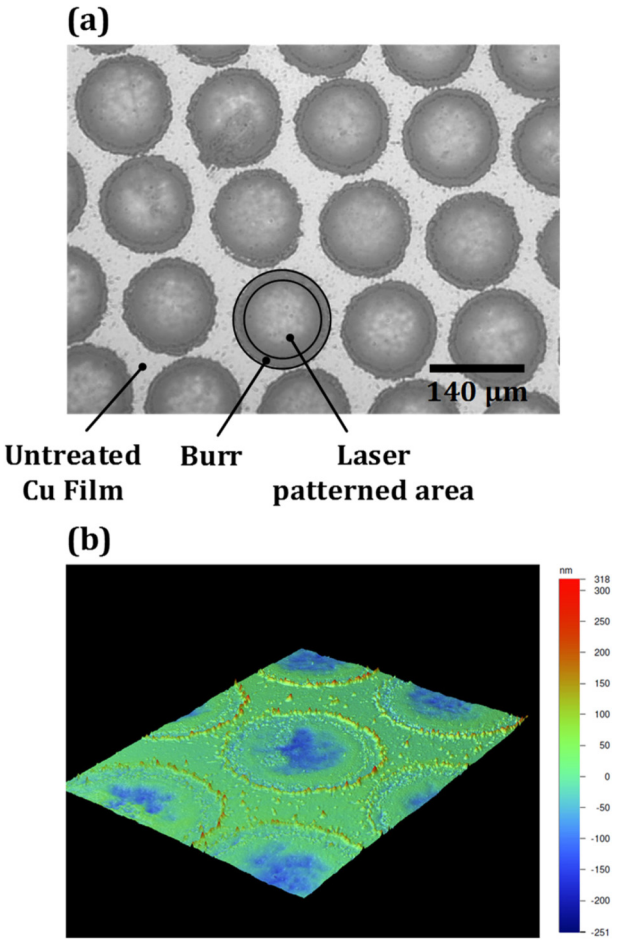

FIG. 7. (a) Optical image and (b) 3D surface profile of the laser-patterned hole array on the 8-nm-thick Cu film with an areal density of 32%.

the laser-patterned film, as shown in Fig. 7(b). It can be found that high laser power intensity caused ejection of condensed and solidified nanoparticle clusters which were deposited around laser-patterned holes. These burrs are neither transparent nor electrically conductive. In the meantime, they will cause scattering effect and increase surface roughness,[34] which may result in poor optical and electrical performance. Slight aperiodicity of the laser-patterned hole array and imperfect hole shape were also observed which could lead to electrical shorts. All of the above-mentioned issues might affect the visible transmittance and electrical conductivity of the laser-patterned film.

IV. DISCUSSION

It is well known that transmittance in the visible wavelength range and electrical conductivity are contradicting properties for all materials. This study has demonstrated the importance of metal film thickness for achieving satisfying visible transmittance and electrical conductivity of the laser-patterned film. As nanosecond laser patterning is a thermal process that experiences melting phase transition, ablating metal film with a thickness on the order of several nanometers will produce a large amount of debris and high surface roughness due to the instability of the melted surface. The excessive surface roughness will result in poor electrical contacts and thus affects the electrical conductivity of the laser-patterned film.[35,36] In addition, the visible transmittance of the as-deposited metal film decreases as the film thickness increases. When the film thickness increases to 28 nm, the average visible transmittance of Cu film decreases to under 8%.[33] Thus, the thickness of the as-deposited metal film should be as low as possible while relatively low sheet resistance should be maintained. Paeng *et al.*[32] also found that the areal density plays a key role in determining the photoelectric properties of the laser-patterned film. In this work, the optimal areal density is 32%. It is believed that the areal density of the laser-patterned film can be further adjusted to achieve the optimal photoelectric performance that can balance visible transmittance and electrical conductivity.

In this work, a significant amount of burrs were found to occur on the periphery of the laser-patterned holes. The laser pulse energy used in this work is on the level of several milliJoules leading to a laser fluence of several tens of J/cm^2, which is much higher than the desired pulse energy and laser fluence (several tens to hundreds of microJoules and ~1 J/cm^2) for laser patterning of hole array on ultrathin metal films. Thus, laser pattering generated a large amount of burrs around the hole circumference. On the contrary, only little amount of burrs were observed when laser patterning the surface using a laser fluence of ~1 J/cm^2.[32] The occurrence of burrs affects the visible transmittance and electrical conductivity of the laser-patterned film. If the burrs can be reduced during laser patterning, the visible transmittance and electrical conductivity of the laser-patterned Cu film can be further increased.

This LMF process for fabrication of transparent conducting films is highly time-efficient and cost-effective. Since a laser beam diameter on the order of several hundreds of micrometers was utilized during laser scanning of the metal thin film in this work, the processing efficiency significantly increases compared with the work done by nanosecond laser,[32] picosecond laser,[37] or femtosecond laser,[38] which used a laser beam diameter on the order of several micrometers. The laser beam diameter could be further increased to several millimeters to enhance the processing efficiency. There are many advantages by using a larger laser beam diameter. On the one hand, the laser fluence used during the laser patterning process will be lower and thus there will be less amount of burrs generated. As a result, the surface roughness of the laser-patterned transparent conducting film can be reduced and the surface quality can be significantly enhanced. On the other hand, the processing time using a laser beam diameter of several millimeters will be at least reduced by more than one hundred times compared with that using a laser beam diameter of several hundred micrometers, which will provide a practical avenue for scaling up the process. Furthermore, it should be noted that this work utilized just a 10 Hz laser with high pulse energy on the level of several milliJoules but it has already significantly increased the process speed compared with the existing work. In Paeng *et al.*,[32] it took more than 4 h to process a 36×36 mm^2 area using their experimental method. In this work, it took around 1 h to fabricate the transparent conducting film with the same area using the optimal laser processing parameters. The process speed can be further significantly increased by using lasers with a higher repetition rate. If a laser at 10 kHz pulse was used, the processing time for the same area could be reduced to 6 s. By utilizing a high frequency laser, as the pulse energy will be much lower compared with that using a low frequency laser, the heat-affected area produced during the laser patterning process will be smaller which helps reduce the amount of burrs generated. In the meantime, this work significantly reduces the production cost by using an affordable nanosecond pulsed laser. It should also be noted that even using laser fluence higher than the desired value, no structural deformation and damage were observed on the glass substrate though the laser-induced temperature had exceeded the glass transition temperature of the glass substrate, demonstrating the practicability of this process. These advantages will render more practical treatment of macroscale transparent substrates, such as glass materials or transparent ceramics to produce transparent conducting surfaces for various optoelectronic applications.[39] For the future work, to further improve the laser-patterned surface quality, rear-side laser patterning will be attempted by placing the substrate deposited with Cu films upside down. In this way, laser will first penetrate through the whole glass substrate and then scan the Cu film at the bottom of the glass substrate. The pulse energy will be decreased before reaching the Cu film and the laser fluence will be reduced. This will help reduce the formation of burrs and protect the glass substrate from being damaged. In addition, the laser power used in the current work remained the same in all experiments; thus, the formation of burrs was the same for all experimental conditions with different areal densities. The relationship between the burr formation and laser processing parameters as well as the effect of burr on photoelectric properties will be of particular interest for future study which will provide more insights into control of burr formation and enhancement of surface quality.

V. CONCLUSIONS

A novel LMF process was developed in this work to enable time-efficient and cost-effective fabrication of large-area transparent conducting films. The laser-patterned ultrathin metal film exhibits

both high transmission in visible spectrum and good electrical conductivity. An average visible transmittance of ~67% and a sheet resistance of ~20 Ω/sq were achieved experimentally, indicating that the transparent conducting film with satisfying photoelectric properties has been successfully fabricated. This laser surface patterning method significantly improves the processing efficiency and reduces production cost compared with the existing methods for fabrication of transparent conducting films. By using an industrial laser, it will render practical treatment of macroscale transparent substrates, such as glass materials or transparent ceramics.

ACKNOWLEDGMENTS

The authors gratefully acknowledge the financial support provided for this study carried out at the University of Iowa by the National Science Foundation under Grant No. #1762353 and the Jiangsu Government Scholarship for Overseas Studies (Reference No. JS-2016-095).

REFERENCES

[1]R. A. Afre, N. Sharma, M. Sharon, and M. Sharon, "Transparent conducting oxide films for various applications: A review," Rev. Adv. Mater. Sci. **53**, 79–89 (2018).
[2]L. Hu, D. S. Hecht, and G. Gruner, "Percolation in transparent and conducting carbon nanotube networks," Nano Lett. **4**, 2513–2517 (2004).
[3]D. Zhang, K. Ryu, X. Liu, E. Polikarpov, J. Ly, M. E. Tompson, and C. Zhou, "Transparent, conductive, and flexible carbon nanotube films and their application in organic light-emitting diodes," Nano Lett. **6**, 1880–1886 (2006).
[4]G. Eda, G. Fanchini, and M. Chhowalla, "Large-area ultrathin films of reduced graphene oxide as a transparent and flexible electronic material," Nat. Nanotechnol. **3**, 270–274 (2008).
[5]K. S. Kim, Y. Zhao, H. Jang, S. Y. Lee, J. M. Kim, K. S. Kim, J. H. Ahn, P. Kim, J. Y. Choi, and B. H. Hong, "Large-scale pattern growth of graphene films for stretchable transparent electrodes," Nature **457**, 706–710 (2009).
[6]H. Hagendorfer, K. Lienau, S. Nishiwaki, C. M. Fella, L. Kranz, A. R. Uhl, D. Jaeger, L. Luo, C. Gretener, S. Buecheler, Y. E. Romanyuk, and A. N. Tiwari, "Highly transparent and conductive ZnO Al thin films from a low temperature aqueous solution approach," Adv. Mater. **26**, 632–636 (2014).
[7]M. Girtan, A. Vlad, R. Mallet, M. A. Bodea, J. D. Pedarnig, A. Stanculescu, D. Mardare, L. Leontie, and S. Antohe, "On the properties of aluminium doped zinc oxide thin films deposited on plastic substrates from ceramic targets," Appl. Surf. Sci. **274**, 306–313 (2013).
[8]H. G. Im, S. H. Jung, J. Jin, D. Lee, J. Lee, D. Lee, J. Y. Lee, I. D. Kim, and B. S. Bae, "Flexible transparent conducting hybrid film using a surface-embedded copper nanowire network: A highly oxidation-resistant copper nanowire electrode for flexible optoelectronics," ACS Nano **8**, 10973–10979 (2014).
[9]J. Y. Lee, S. T. Connor, Y. Cui, and P. Peumans, "Solution-processed metal nanowire mesh transparent electrodes," Nano Lett. **8**, 689–692 (2008).
[10]P. B. Catrysse and S. Fan, "Nanopatterned metallic films for use as transparent conductive electrodes in optoelectronic devices," Nano Lett. **10**, 2944–2949 (2010).
[11]D. Lee, D. Paeng, H. K. Park, and C. P. Grigoropoulos, "Vacuum-free, maskless patterning of Ni electrodes by laser reductive sintering of Nio nanoparticle ink and its application to transparent conductors," ACS Nano **8**, 9807–9814 (2014).
[12]M. S. Lee, K. Lee, S. Y. Kim, H. Lee, J. Park, K. H. Choi, H. K. Kim, D. G. Kim, D. Y. Lee, S. Nam, and J. U. Park, "High-performance, transparent, and stretchable electrodes using graphene-metal nanowire hybrid structures," Nano Lett. **13**, 2814–2821 (2013).
[13]S. Ye, A. R. Rathmell, Z. Chen, I. E. Stewart, and B. J. Wiley, "Metal nanowire networks: The next generation of transparent conductors," Adv. Mater. **26**, 6670–6687 (2014).
[14]S. Hong, J. Yeo, G. Kim, D. Kim, H. Lee, J. Kwon, H. Lee, P. Lee, and S. H. Ko, "Nonvacuum, maskless fabrication of a flexible metal grid transparent conductor by low-temperature selective laser sintering of nanoparticle ink," ACS Nano **7**, 5024–5031 (2013).
[15]H. Wu, D. Kong, Z. Ruan, P.-C. Hsu, S. Wang, Z. Yu, T. J. Carney, L. Hu, S. Fan, and Y. Cui, "A transparent electrode based on a metal nanotrough network," Nat. Nanotechnol. **8**, 421–425 (2013).
[16]J. A. Jeong, H. K. Kim, and J. Kim, "Invisible Ag grid embedded with ITO nanoparticle layer as a transparent hybrid electrode," Sol. Energy Mater. Sol. Cells **125**, 113–119 (2014).
[17]C. T. Wang, C. C. Ting, P. C. Kao, S. R. Li, and S. Y. Chu, "Investigation of surface energy, polarity, and electrical and optical characteristics of silver grids deposited via thermal evaporation method," Appl. Surf. Sci. **360**, 349–352 (2016).
[18]J. Y. Kim, J. S. Park, J. Y. Na, S. K. Kim, D. Kang, and T. Y. Seong, "Using agglomerated Ag grid to improve the light output of near ultraviolet AlGaN-based light-emitting diode," Microelectron. Eng. **169**, 29–33 (2017).
[19]M.-G. Kang and L. J. Guo, "Nanoimprinted semitransparent metal electrodes and their application in organic light-emitting diodes," Adv. Mater. **19**, 1391–1396 (2007).
[20]B. Li, L. Huang, M. Zhou, N. Ren, and B. Wu, "Surface morphology and photoelectric properties of fluorine-doped tin oxide thin films irradiated with 532 nm nanosecond laser," Ceram. Int. **40**, 1627–1633 (2014).
[21]B. J. Li, M. Zhou, M. Ma, W. Zhang, and W. Y. Tang, "Effects of nanosecond laser irradiation on photoelectric properties of AZO/FTO composite films," Appl. Surf. Sci. **265**, 637–641 (2013).
[22]L. Huang, N. Ren, B. Li, and M. Zhou, "A comparative study of different M (M=Al, Ag, Cu)/FTO bilayer composite films irradiated with nanosecond pulsed laser," J. Alloys. Compd. **617**, 915–920 (2014).
[23]L. J. Huang, N. F. Ren, B. J. Li, and M. Zhou, "Improvement in overall photoelectric properties of Ag/FTO bilayer thin films using furnace/laser dual annealing," Mater. Lett. **116**, 405–407 (2014).
[24]N. F. Ren, L. J. Huang, B. J. Li, and M. Zhou, "Laser-assisted preparation and photoelectric properties of grating-structured Pt/FTO thin films," Appl. Surf. Sci. **314**, 208–214 (2014).
[25]B. J. Li, L. J. Huang, N. F. Ren, and M. Zhou, "Titanium dioxide-coated fluorine-doped tin oxide thin films for improving overall photoelectric property," Appl. Surf. Sci. **290**, 80–85 (2014).
[26]N. F. Ren, L. J. Huang, M. Zhou, and B. J. Li, "Introduction of Ag nanoparticles and AZO layer to prepare AZO/Ag/FTO trilayer films with high overall photoelectric properties," Ceram. Int. **40**, 8693–8699 (2014).
[27]L. J. Huang, N. F. Ren, B. J. Li, and M. Zhou, "Effect of annealing on the morphology, structure and photoelectric properties of AZO/Pt/FTO trilayer films," Acta Metall. Sin. (English Lett.) **28**, 281–288 (2015).
[28]L. J. Huang, N. F. Ren, B. J. Li, and M. Zhou, "Ni/FTO bilayer thin films with high photoelectric properties optimized by magnetic-field-assisted laser annealing," Mater. Lett. **140**, 75–78 (2015).
[29]B. J. Li, L. J. Huang, N. F. Ren, X. Kong, Y. L. Cai, and N. L. Zhang, "Two-step preparation of laser-textured Ni/FTO bilayer composite films with high photoelectric properties," J. Alloys Compd. **640**, 376–382 (2015).
[30]B. Li, L. Huang, N. Ren, X. Kong, Y. Cai, and J. Zhang, "Improving the performance of nickel-coated fluorine-doped tin oxide thin films by magnetic-field-assisted laser annealing," Appl. Surf. Sci. **351**, 113–118 (2015).
[31]L. J. Huang, B. J. Li, and N. F. Ren, "Enhancing optical and electrical properties of Al-doped ZnO coated polyethylene terephthalate substrates by laser annealing using overlap rate controlling strategy," Ceram. Int. **42**, 7246–7252 (2016).
[32]D. Paeng, J. H. Yoo, J. Yeo, D. Lee, E. Kim, S. H. Ko, and C. P. Grigoropoulos, "Low-cost facile fabrication of flexible transparent copper electrodes by nanosecond laser ablation," Adv. Mater. **27**, 2762–2767 (2015).

[33]E. Shahriari and M. G. Varnamkhasti, "Nonlinear optical and electrical characterization of nanostructured Cu thin film," Superlattices Microstruct. **75**, 523–532 (2014).
[34]R.Bhadresha, J. Sukham, A. Pattanayak, G. Rana, P. Deshmukh, S. P. Duttagupta, N. Sarwade, G. Jacob, and S. S. Prabhu, "THz bandpass filter based on sub-wavelength holes in free-standing metal thin-films," in *2015 40th International Conference on Infrared, Millimeter, and Terahertz Waves (IRMMW-THz), Hong Kong, 23–28 August 2015* (IEEE, New York, 2015), pp. 11–12.
[35]D. W. Bäuerle, *Laser Processing and Chemistry* (Springer, Berlin, 2011).
[36]W. Steen and J. Mazumder, *Laser Material Processing* (Springer, London, 2010).
[37]M. Domke, L. Nobile, S. Rapp, S. Eiselen, J. Sotrop, H. P. Huber, and M. Schmidt, "Understanding thin film laser ablation: The role of the effective penetration depth and the film thickness," Phys. Procedia **56**, 1007–1014 (2014).
[38]J. Kim and S. Na, "Metal thin film ablation with femtosecond pulsed laser," Opt. Laser. Technol. **39**, 1443–1448 (2007).
[39]S. F. Wang, J. Zhang, D. W. Luo, F. Gu, D. Y. Tang, Z. L. Dong, G. E. B. Tan, W. X. Que, T. S. Zhang, S. Li, and L. B. Kong, "Transparent ceramics: Processing, materials and applications," Prog. Solid State. Chem. **41**, 20–54 (2013).